International Journal of Medical, Medicine and Health Sciences
ISSN: 2517-9969
Vol:6, No:6, 2012

Computational Analysis of Hemodynamic Effects on Aneurysm Coil Bundle

Woowon Jeong, Kyehan Rhee

***Abstract*—**Recurrence of aneurysm rupture can be attributed to coil migration and compaction. In order to verify the effects of hemodynamics on coil compaction and migration, we analyze the forces and displacements on the coil bundle using a computational method. Lateral aneurysms partially filled coils are modeled, and blood flow fields and coil deformations are simulated considering fluid and solid interaction. Effects of aneurysm neck size and parent vessel geometry are also investigated. The results showed that coil deformation was larger in the aneurysms with a wider neck. Parent vessel geometry and aneurysm neck size also affected mean pressure force profiles on the coil surface. Pressure forces were higher in wide neck models with curved parent vessel geometry. Simulation results showed that coils in the wide neck aneurysm with a curved parent vessel may be displaced and compacted more easily.

***Keywords*—**Hemodynamics, Aneurysm, Coil compaction, Fluid Structure Interaction (FSI)

I. Introduction

CEREBRAL aneurysm is a vascular disease characterized by local dilatation of the arterial wall in the intracranial space. It may rupture and cause subarachnoid hemorrhage, which is associated with high mortality and morbidity [1]-[3]. Endovascular treatment of saccular aneurysms with Guglielmi detachable coils (GDC) has been used as a prophylactic treatment since early 1990s. Coils packed into the aneurysm sac induce flow stasis and thrombus formation [4]-[6]; therefore, completely obliterate the aneurysm sac. However, recurrence of subarachnoid hemorrhage after coiling has been reported [7], [8]. The aneurysm recanalization can be attributed to coil compaction and aneurysm regrowth [9]. Complete filling of aneurysm sac with coils are difficult, and coil packing density, which is defined as the ratio between the volume of inserted coil and aneurysm, higher than 20% has been recommended to prevent coil compaction [10]. Compaction of the coil is related to the deformation and migration of coils due to the hemodynamic forces.

Hemodynamic analyses of aneurysm filled with coils have been performed by previous researchers. Hemodynamics of partially blocked aneurysms was analyzed by using a computational fluid dynamic (CFD) method [11], [12]. Intra-aneurysmal hemodynamics was computationally investigated by modeling coils as a porous medium [13], [14]. Thromboembolization inside of coils was simulated using the viscosity model defined as a function of both residence time and clotting fluid concentration [15]. Most of previous aneurismal hemodynamic studies focused on the flow patterns, intra-aneurismal flow and vessel wall shear stress in order to elucidate the hemodynamic role of thromboembolization and aneurysm regrowth.

Woowon Jeong is with Myongji University, Yongin, Gyeonggido, South Korea

Kyehan Rhee was with Myongji University, Yongin, Gyeonggido, South Korea (phone: 82-31-3306426; fax: 82-31-3306957; e-mail: khanrhee@mju.ac.kr)

Coil compaction and migration is one of the major causes of aneurysm recanalization, but hemodynamic study on coil compaction has not been performed. In this study, we analyze the forces and deformations on the coil bundle caused by blood flow in order to verify the effects of hemodynamics on coil compaction and migration. Effects of aneurysm neck size and parent vessel geometries on coil compaction and migration are also explored.

II. Methods

A. Aneurysm models

The lateral aneurysm models in the intracranial space were modeled in this study. Pear shaped saccular aneurysms were formed on the lateral side of a straight and a curved parent vessels. Since the size and shape of aneurysms of cerebral artery are different for individuals, the average values of aneurysm sac and internal carotid artery sizes, which were measured and analyzed statistically [16], were used. The dome diameter, dome height, and parent artery diameter of pear aneurysms were 5.3, 4.3 and 3.6 mm. In order to estimate the effect of aneurysm neck size, the neck size was 4 mm (normal) and 5.3 (wide) mm. For curved parent vessel the ratio of the parent vessel diameter to the radius of curvature was 0.17. The coil was modeled as a sphere, and the inserted coils were assumed to be densely packed. The diameter of a sphere is 95% of aneurysm dome diameter.

B. Numerical Analysis

Numerical analysis was performed using a commercial finite element package (ADINA 8.5, Watertown, MA) which is a capable of solving the fully coupled fluid structure interaction (FSI) problems. The governing finite element equations for both the solid and fluid models were solved by Newton-Raphson iteration method. Blood was assumed to be incompressible, laminar flow. The density of blood was 1060 kg/m^3. The non-Newtonian viscosity characteristics of blood were incorporated by using the Carreau model, which was expressed as follows [17]:

$$\eta = \eta_\infty + (\eta_0 - \eta_\infty)\left[1+\lambda^2\gamma^2\right]^{\left(\frac{q-1}{2}\right)} \quad (1)$$

where rheological values of human blood are η_0 = 0.056Pa·s, η_∞ = 0.00345Pa·s, λ= 3.313s, q= 0.356. η is viscosity, γ is shear rate.

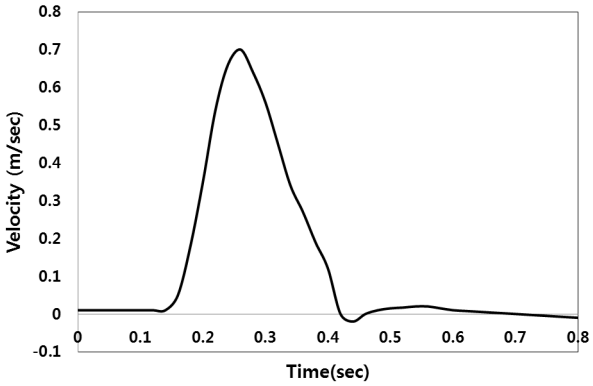

Fig. 1 Area average velocity at the inlet of a parent vessel during a flow cycle

The solid domain was treated as linear elastic with Young's modulus of 3 and 5 kPa. Poisson's ratio was 0.35 and density was 1060 kg/m^3 [18]. The element size of fluid and solid was 0.1 mm, 4-node and 8-node rectangular elements were used. Further refinement of grid did not affect the computational results. The coil was modeled as the solid using the formulation with large displacement and small strains in the FSI calculation. Continuity and Navier-Stokes equations were solved for the fluid. Wall boundary conditions were imposed on the vessel walls. Parabolic velocity profiles were applied at the inlet boundary, and normal traction condition were applied at the outlet boundary. A physiological flow waveform was used [11]. The area average velocity profile at the inlet of the parent vessel for a flow cycle is shown in Fig. 1. Unsteady simulations were performed with the time step size of 0.002 s, and the solution was converged after three flow cycles. Computations were performed using 3.4 GHz Intel core CPU and 16 GB of RAM with Window 7 64 bit operating system.

III. Results

In order to estimate coil compaction caused by hemodynamic force, coil area changes were calculated. The coil area reduction was calculated by dividing the reduced coil area by the undeformed coil area. The coil area reductions during a flow cycle are shown in Fig. 2. The maximum reductions of coil area in the straight parent vessel models were less than 1.5% and 3% in the normal and wide-neck models, respectively. In the curved parent vessel models, the maximum reductions of coil area were less than 8.5% and 8% in the normal and wide-neck models, respectively. Coils in the curved parent vessel model exhibited more deformation, which was probably due to the high inflow and pressure forces caused by centrifugal force. The effect of aneurysm neck size on coil deformation was large in the straight parent vessel model but not significant in the curved parent vessel model. Mean pressure force on the coil surface (MPF) was calculated because it might be related to coil compaction. Coil elasticity did not affect the MPF significantly, but aneurysm neck size and parent vessel geometry affected the MPF profile (Fig. 3). MPFs were higher in wide neck model comparing to those in regular neck model, and they showed significant difference in the straight parent vessel model comparing to the curved parent vessel model.

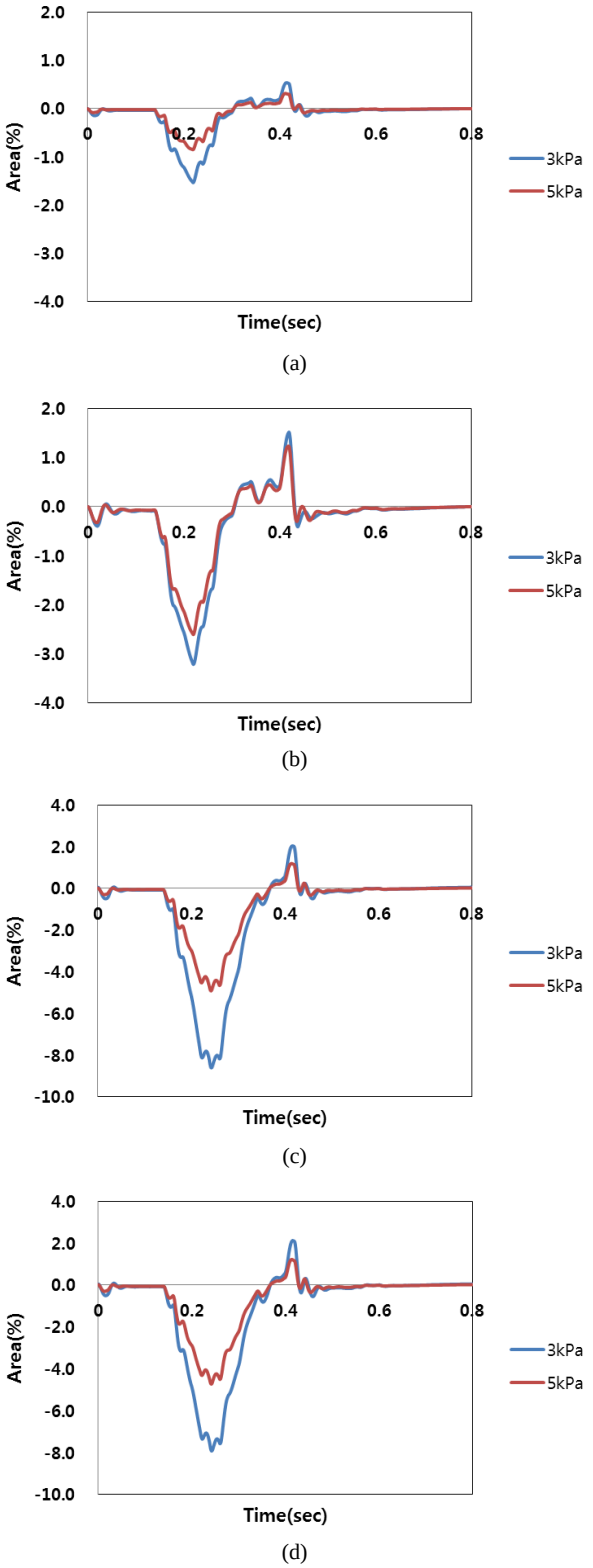

Fig. 2 Area changes of the coil on parent vessel geometries: (a) 4mm neck of a straight parent vessel, (b) 5.3mm neck of a straight parent vessel (c) 4mm neck of a curved parent vessel (d) 5.3mm neck of a curved parent vessel

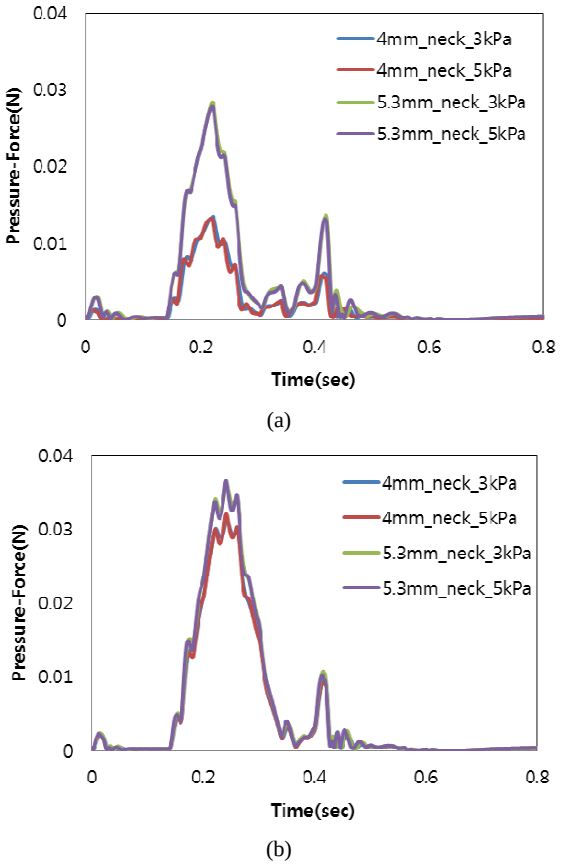

Fig. 3 Mean pressure force on the coil surface: (a) Straight parent vessel, (b) Curved parent vessel

The time-averaged mean kinetic energy (MKE) inside the aneurysm was calculated. The MKEs were highest in the no-coil model and the lowest in the rigid model as shown in Fig. 4. MKEs of the normal and wide-neck no-coil models with the straight parent vessel models were about 13 and 6.7 times of those in the rigid coil. In the curved parent vessel models, MKEs of the normal and wide-neck no-coil models were about 10 and 6 times of those in the rigid coil. MKEs were higher in the elastic coil models than in the rigid models. Moreover, the elastic coil model with the lower Young's modulus showed a higher MKE in aneurysm sac.

Computational results show that coil area reduction is higher in elastic coil model; therefore elastic coil models are more prone to be compacted. The aneurysm neck size and parent vessel geometry influences the pressure force significantly; therefore, coils in the wide neck aneurysms with a curved parent vessel might experience more coil compaction.

IV. Conclusions

Incomplete filling of coils inside of the aneurysm sac causes coil migration and compaction, and they may be related to the hemodynamic forces. In order to investigate these effects, computational analyses on coil deformation caused by hemodynamic force were performed in the lateral aneurysm models with coils. Computational methods considering fluid structure interactions were employed. Simulation results showed that parent vessel geometry and coil elasticity affected coil deformation. Kinetic energy was highest in the no-coil model and the lowest in the rigid coil model. Hemodynamics in aneurysm was affected by coil elasticity, aneurysm neck size, and parent vessel geometry; therefore, elastic coils in the wide neck aneurysm with a curved parent vessel may be displaced and compacted more easily.

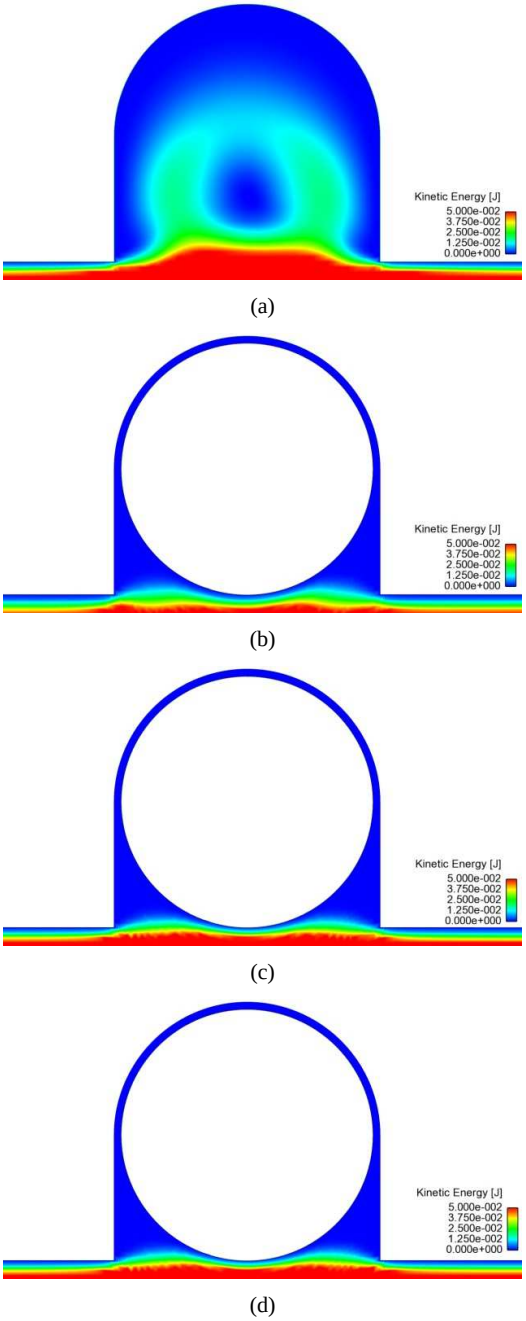

Fig. 4 The kinetic energy contour at 0.5sec: (a) no-coil (b) rigid coil bundle (c) Young's modulus of 3kPa coil bundle (d) Young's modulus of 5kPa coil bundle

ACKNOWLEDGMENT

This study was supported by a grant from the Korean Health Technology R&D Project, Ministry of Health and Welfare, Republic of Korea (A111101).

REFERENCES

[1] M. Kaminogo, M. Yonekura, and S. Shibata, "Incidence and outcome of multiple intracranial aneurysms in a defined population," *Stroke*, vol. 34, pp. 16-21, 2003.
[2] F. H. H. Linn, G. J. E. Rinkel, A. Algra, and J. Van Gijn, "Incidence of subarachnoid hemorrhage: role of region, year, and rate of computed tomography: a meta-analysis," *Stroke*, vol. 27, pp. 625-629, 1996.
[3] H. R. Winn, J. A. Jane, J. Taylor, D. Kaiser, and G. W. Britz, "Prevalence of asymptomatic incidental aneurysms: review of 4568 arteriograms," *Journal of neurosurgery*, vol. 96, pp. 43-49, 2002.
[4] C. Groden, J. Laudan, S. Gatchell, and H. Zeumer, "Three-dimensional pulsatile flow simulation before and after endovascular coil embolization of a terminal cerebral aneurysm," *Journal of Cerebral Blood Flow & Metabolism*, vol. 21, pp. 1464-1471, 2001.
[5] S. I. Stiver, P. J. Porter, R. A. Willinsky, and M. C. Wallace, "Acute human histopathology of an intracranial aneurysm treated using Guglielmi detachable coils: case report and review of the literature," *Neurosurgery*, vol. 43, pp. 1203-1208, 1998.
[6] H. Tenjin, S. Fushiki, Y. Nakahara, H. Masaki, T. Matsuo, C. M. Johnson, and S. Ueda, "Effect of Guglielmi detachable coils on experimental carotid artery aneurysms in primates," *Stroke*, vol. 26, pp. 2075-2080, 1995.
[7] A. J. Molyneux, R. S. C. Kerr, J. Birks, N. Ramzi, J. Yarnold, M. Sneade, and J. Rischmiller, "Risk of recurrent subarachnoid haemorrhage, death, or dependence and standardised mortality ratios after clipping or coiling of an intracranial aneurysm in the International Subarachnoid Aneurysm Trial (ISAT): long-term follow-up," *The Lancet Neurology*, vol. 8, pp. 427-433, 2009.
[8] J. Raymond, F. Guilbert, A. Weill, S. A. Georganos, L. Juravsky, A. Lambert, J. Lamoureux, M. Chagnon, and D. Roy, "Long-term angiographic recurrences after selective endovascular treatment of aneurysms with detachable coils," *Stroke*, vol. 34, pp. 1398-1403, 2003.
[9] J. Raymond, T. Darsaut, I. Salazkin, G. Gevry, and F. Bouzeghrane, "Mechanisms of occlusion and recanalization in canine carotid bifurcation aneurysms embolized with platinum coils: an alternative concept," *American journal of neuroradiology*, vol. 29, pp. 745-752, 2008.
[10] Y. Kawanabe, A. Sadato, W. Taki, and N. Hashimoto, "Endovascular occlusion of intracranial aneurysms with Guglielmi detachable coils: correlation between coil packing density and coil compaction," *Acta neurochirurgica*, vol. 143, pp. 451-455, 2001.
[11] S. Ahmed, I. D. Sutalo, H. Kavnoudias, and A. Madan, "numerical investigation of hemodynamics of lateral cerebral aneurysm following coil embolization," *Engineering Applications of Computational Fluid Mechanics*, vol. 5, pp. 329-340, 2011.
[12] H. S. Byun and K. Rhee, "CFD modeling of blood flow following coil embolization of aneurysms," *Medical engineering & physics*, vol. 26, pp. 755-761, 2004.
[13] N. M. P. Kakalis, A. P. Mitsos, J. V. Byrne, and Y. Ventikos, "The haemodynamics of endovascular aneurysm treatment: a computational modelling approach for estimating the influence of multiple coil deployment," *Medical Imaging, IEEE Transactions on*, vol. 27, pp. 814-824, 2008.
[14] A. P. Mitsos, N. M. P. Kakalis, Y. P. Ventikos, and J. V. Byrne, "Haemodynamic simulation of aneurysm coiling in an anatomically accurate computational fluid dynamics model: technical note," *Neuroradiology*, vol. 50, pp. 341-347, 2008.
[15] A. Narracott, S. Smith, P. Lawford, H. Liu, R. Himeno, I. Wilkinson, P. Griffiths, and R. Hose, "Development and validation of models for the investigation of blood clotting in idealized stenoses and cerebral aneurysms," *Journal of Artificial Organs*, vol. 8, pp. 56-62, 2005.
[16] L. Parlea, R. Fahrig, D. W. Holdsworth, and S. P. Lownie, "An analysis of the geometry of saccular intracranial aneurysms," *American journal of neuroradiology*, vol. 20, p. 1079, 1999.
[17] Y. I. Cho and K. R. Kensey, "Effects of the non-Newtonian viscosity of blood on flows in a diseased arterial vessel. Part 1: Steady flows," *Biorheology*, vol. 28, p. 241, 1991.
[18] G. Finet, J. Ohayon, and G. Rioufol, "Biomechanical interaction between cap thickness, lipid core composition and blood pressure in vulnerable coronary plaque: impact on stability or instability," *Coronary artery disease*, vol. 15, p. 13, 2004.